

fastHDMI: Fast Mutual Information Estimation for High-Dimensional Data

Kai Yang^{1*}, Masoud Asgharian¹, Nikhil Bhagwat^{1, 3},
Jean-Baptiste Poline¹, Celia Greenwood^{1, 2}

^{1*}McGill University, Montreal, Quebec, Canada.

^{2*}Lady Davis Institute for Medical Research, Jewish General Hospital,
Montreal, Quebec, Canada.

^{3*}Origami Lab, Montreal Neurological Institute, McGill University,
Montreal, Quebec, Canada.

*Corresponding author(s). E-mail(s): kai.yang2@mail.mcgill.ca;
Contributing authors: masoud.asgharian2@mcgill.ca;
nikhil.bhagwat@mcgill.ca; jean-baptiste.poline@mcgill.ca;
celia.greenwood@mcgill.ca;

Abstract

In this paper, we introduce **fastHDMI**, a Python package for the efficient execution of variable screening for high-dimensional datasets, including neuroimaging datasets. This study marks the inaugural application of three distinct mutual information estimation methodologies for variable selection in the context of neuroimaging analysis, a novel contribution implemented through **fastHDMI**. Such advancements are critical for dissecting the complex architectures inherent in neuroimaging datasets, offering refined mechanisms for variable selection against the backdrop of high dimensionality. Employing the preprocessed Autism Brain Imaging Data Exchange (ABIDE) dataset [6, 2] as a foundation, we assess the efficacy of these variable screening methodologies through extensive simulation studies. These evaluations encompass a diverse set of conditions, including linear and nonlinear associations, alongside continuous and binary outcomes. The results delineate the *Fast Fourier Transform Kernel Density Estimation (FFTKDE)*-based mutual information estimation approach as preeminent for feature screening with continuous nonlinear outcomes, while the binning-based methodology is identified as superior for binary outcomes contingent on nonlinear underlying probability preimage. For linear simulations, a parity in performance is observed for continuous outcomes between the absolute Pearson correlation

and FFKDE-based mutual information estimation, with the former also exhibiting dominance in binary outcomes predicated on linear underlying probability preimage. A comprehensive case analysis utilizing the preprocessed Autism Brain Imaging Data Exchange (ABIDE) dataset further illuminates the applicative potential of **fastHDMI**, demonstrating the predictive capabilities of models constructed from variables selected through our implemented screening methods. This research not only substantiates the computational prowess and methodological robustness of **fastHDMI**, but also contributes significantly to the arsenal of analytical tools available for neuroimaging research.

Keywords: keyword1, Keyword2, Keyword3, Keyword4

1 Introduction

The question of how to best select a subset of variables from a large set is a commonly investigated topic in high-dimensional model fitting [9]. This topic is often called “variable selection” in statistics, or “feature selection” in the machine learning world. Feature selection may be necessary either to fit a particular statistical model or, in some situations, because the data are too large for memory. Neuroimaging data provide a good example of such challenges. For example, Magnetic Resonance Images (MRI) result in measurements at millions of voxels [3, 34, 36, 17], and the development of multiple imaging modalities is leading to multiple high-dimensional sets of features, each capturing a different aspect of brain function, that can show widespread correlation patterns within and between each modality. These high dimensions in neuroimaging data have stimulated the development of variable selection methods; indeed, there has been a recent surge in publications: see, for example, [1, 17, 18, 22, 23, 24, 25, 27, 40, 39, 45, 49, 50, 54, 58]. These papers take a wide variety of strategies ranging from univariate to multivariate selection. Among these, Fan and Chou, Schlögl et al. [17, 50] considered absolute correlation or mutual information with respect to the outcome as a conventional univariate approach; selection based on sparse-inducing penalties on multi-variable models were proposed on the data [17, 23, 25, 49] or transformed data [1]. Multivariate selection based on random forest variable importance [18, 23] or sign consistency from the support vector machine [22] has also been applied previously. A “potential support vector machine” was applied by Mohr et al. [40], an idea that rests on exchanging the roles of data points and features. Another approach can be seen in [39], where they selected features recursively based on multivariate model fitting. Evidently, these papers take a wide variety of strategies ranging from simple methods like analyzing the direct absolute correlation between outcomes and features, to more complex approaches involving the use of univariate regression coefficients, univariate copulas, and techniques that leverage variable importance measures or sparse penalties in multivariate model fitting. Variable selection under a multivariable model generally requires certain assumptions, often including the assumption of linearity, which is not robust to misspecification. Furthermore, variable selection based on marginal associations demands less computational power and memory and can easily adapt to

data inflow. Additionally, variable selection within a joint model framework allows for variable screening conditioned on other covariates, such as confounders.

Although Pearson correlation is frequently used to measure the association between covariates and the outcome, in situations where nonlinearity may be present, a variety of strategies have been introduced to examine the relationship between the outcome and the covariates [47, 48, 55]. These methods, when utilized for feature screening, effectively equate to screening via mutual information, as they are all deterministic monotonically increasing functions of mutual information. Among the strategies for feature selection, an entropy-based method, *mutual information* has two appealing characteristics. As defined in (3), mutual information is defined as the Kullback–Leibler divergence (KL divergence) between the joint distribution of two variables and their outer product distribution, effectively quantifying their dependency. This method can carry out model-independent feature selection, and is robust to non-linearity between the outcome and the features. For these reasons, mutual information has already been a popular choice for neuroimaging data. Ince et al. [26] proposed to estimate mutual information based on the Gaussian Copula for continuous data, which works well for approximately Gaussian data, such as local field potentials and M/EEG data [38]. Nemirovsky et al. [42] advanced the analysis of functional MRI data by implementing integrated information theory, which is calculated based on the mutual information between the state of the conscious system over time and across the conscious system’s partitions. Tsai et al. [59] used mutual information to analyze functional MRI data to compute an activation map. Schlögl et al. [50] used mutual information to study the EEG-based brain-computer interface. Chai et al. [8] and Li [33] employed multivariate mutual information to study functional connectivity between brain regions in functional MRI data. Combrisson et al. [12] proposed a nonparametric permutation-based framework for neurophysiological data to analyze cognitive brain networks.

While mutual information estimation for discrete random variables is trivial, the estimation of mutual information for continuous random variables can be done using a few different approaches. One fundamental method is to estimate mutual information based on the binning of continuous variables to treat them as discrete variables. Steuer et al. [57] reported improved performance using Kernel Density Estimation (KDE) based methods. KDE-based methods numerically calculate the mutual information estimation based on the estimated kernel density functions [41]. The k -Nearest Neighbors (k NN) approach was previously adapted to estimate mutual information [16, 31, 60, 44, 37, 21]. Khan et al. [30] compared the performance of mutual information estimators based on k NN and KDE and concluded that KDE-based mutual information estimators outperform k NN-based estimators for small samples with a high noise level. Gao et al. [21] argued that accurate estimation of mutual information of two strongly dependent variables using k NN-based methods requires a prohibitively large sample size. As shown later in our simulation studies in Section 3.1, our KDE-based mutual information screening method also outperforms the k NN-based counterpart. Since kernel density estimation on large volume of data is a computationally challenging approach and that neuroimaging data is usually of large volume, variable

screening based on mutual information has never been implemented for neuroimaging data to the best of our knowledge. In this paper, we implement variable screening methods using a few different approaches and carried out comprehensive simulation and real case studies using the preprocessed ABIDE data [6, 2]. The variable screening functionality is encapsulated within our Python package, `fastHDMI`, an acronym for *Fast high-dimensional Mutual Information estimation*. This package is specifically designed to facilitate the effective processing and analysis of substantial volumes of neuroimaging data using a few different computationally efficient estimation methods.

In Section 2, we will explore the concept of mutual information and provide an overview of the estimation methods. Subsequently, Section 3 assesses the efficacy of variable selection and the computational speed of the variable selection methods implemented in our `fastHDMI` package. These methods encompass *Fast Fourier Transform-based Kernel Density Estimation (FFTKDE)* mutual information estimation, mutual information estimation based on binning of continuous variables with the number of bins determined using the results of a previous study [4] utilizing bounds on the risk of penalized maximum likelihood estimators due to Castellán [7], *k*NN-based mutual information estimation, and Pearson correlation. The *k*NN-based mutual information estimation utilized in our work is adapted from the `scikit-learn` library. We will begin by examining these variable screening methods within our `fastHDMI` package through simulations in Section 3.1, then proceed to compare their computing speeds. Finally, in Section 3.2, the performance of the predictive models created with the variables selected using our four implemented methods will be demonstrated.

2 Estimation of Mutual Information

The entropy-based screening methods are based on Shannon’s entropy [51]. Let $\mathbf{X} \in \mathbb{R}^n$ denote a random variable residing in a probability space with probability mass or density function $p(\mathbf{X})$. Shannon’s entropy is defined as

$$H(\mathbf{X}) := \mathbb{E}[-\log p(\mathbf{X})]. \quad (1)$$

Furthermore, Lebesgue’s decomposition theorem expands the above definition for all other random variables. Relative entropy, also known as the *KL divergence*, is a specific case of Bregman divergence applied to $-H$, the negative of Shannon’s entropy, which is a strictly convex functional:

$$D_{KL}(\mathbf{X}_1 \parallel \mathbf{X}_2) := \mathbb{E}_{\mathbf{X}_1} \left[-\log \frac{p(\mathbf{X}_2)}{p(\mathbf{X}_1)} \right]. \quad (2)$$

Moreover, mutual information is defined as the KL divergence from the joint distribution (\mathbf{X}, \mathbf{Y}) to the outer product distribution $\mathbf{X} \otimes \mathbf{Y}$, hence symmetric. For random variables \mathbf{X}, \mathbf{Y} , the mutual information

$$I(\mathbf{X}, \mathbf{Y}) := D_{KL}((\mathbf{X}, \mathbf{Y}) \parallel \mathbf{X} \otimes \mathbf{Y}). \quad (3)$$

\mathbf{X} and \mathbf{Y} in (3) are typically univariate for variable screenings. The implementation of KDE-based mutual information estimation uses Fast Fourier Transform (FFT) based KDE methods from the Python package `KDEpy` [43]. FFT-based KDE was initially proposed by Silverman [53] on Gaussian kernels with much faster computing speed and much lower numerical errors. As shown in the paper, such an approach significantly solves the computational speed challenges that KDE usually faces [53]. The performance of KDE usually depends on the bandwidth and kernel selection. While we leave it for users to choose kernel and bandwidth, the default arguments are set to be the state-of-the-art *Improved Sheather-Jones* bandwidth [5] with Epanechnikov kernel [15]. For a detailed explanation of the FFTKDE method for mutual information estimation, see Appendix A.

At the same time, mutual information estimation using the k NN method leverages the k NN algorithm for entropy estimation, a technique introduced by L. F. Kozachenko [32]. This method estimates Shannon entropy, as detailed in equation (1), with the sample mean, alongside a trinomial distribution to estimate $\widehat{p}(x_j)$. The binning approach for mutual information estimation converts continuous variables into discrete variables through binning, with the optimal number of bins guided by findings from a previous study by Birgé and Rozenholc [4], which derived the optimal number of bins based on the bounds on the risk of penalized maximum likelihood estimators due to Castellán [7]. Pearson correlation is calculated through the standardized inner product of outcomes and variables. Additionally, to drastically improve the processing speed for large-scale datasets, our package incorporates multiprocessing capabilities, enabling parallel processing across all employed methods. This adaptation to parallel computing significantly enhances the utility of our package, especially for extensive neuroimaging data analyses.

Previous studies demonstrated that the three density estimation methods discussed in this paper, KDE, k NN, and histogram-based methods, are consistent estimators under suitable conditions. The Lebesgue integral, as a linear operator, has its boundedness equivalent to continuity in a normed linear space. Since expectation is a linear operator, it is continuous under appropriate norms when it is bounded. By the continuous mapping Theorem, the mutual information estimated using these three density estimators is consistent, as the mutual information functional is continuous with respect to the joint likelihood, and continuity is preserved under finite composition.

Furthermore, since mutual information is continuous with respect to the joint density, sufficiently small numerical errors will not significantly perturb the mutual information estimation. The numerical error associated with the FFT procedure arises from multiple sources beyond numerical precision, including errors from using a finite number of Discrete Fourier Transform (DFT) terms — such as discretization, truncation of frequencies, and aliasing; and errors from applying FFT to a non-periodic function, including boundary effects, zero-padding, and interpolation. Notably, Fourier’s theorem implies that the error from FFT for *periodic* functions vanishes asymptotically with respect to the number of DFT terms. With a computational complexity of $O(n \log n)$, utilizing a sufficiently fine grid can mitigate these errors while maintaining high computational efficiency. Moreover, KDE is inherently

non-periodic. Consequently, errors due to boundary effects, zero-padding, and interpolation are influenced by the chosen interval for KDE and will not asymptotically vanish with respect to the number of DFT terms. The error due to the chosen bounded interval in which the data points reside presents a general challenge when evaluating mutual information numerically, not limited to the FFT approach. Additionally, it is important to note that numerical errors, though generally insignificant when using a large number of DFT terms, will not vanish asymptotically with respect to the number of data points in the dataset. In summary, FFT is an efficient tool to perform KDE while maintaining high computational efficiency, as evidenced by previous studies [53].

3 Simulation and Case Studies

Autism Brain Imaging Data Exchange (ABIDE) preprocessed Data consists of preprocessed functional MRI brain imaging data from 539 individuals suffering from ASD and 573 typical controls [6]. In this paper, we used the preprocessed ABIDE data consisting of 149955 brain imaging variables, together with age, biological sex, and diagnosis of autism for 508 cases and 542 controls [6, 2]. The preprocessing was carried out exactly the same manner as the preprocessing performed earlier by Barry et al. [2] (see also [19, 14]): the T1-weighted Magnetic Resonance scans were processed through the FreeSurfer 6.0 pipeline [19] on the CBrain computing facility [52]. This pipeline delineates the cortical surface from magnetic resonance scans, allowing the quantification of the cortical thickness across the brain hemispheres [19, 14]. The process involves several steps: affine registration to MNI305 space [11], bias field correction, removal of non-cortical regions, and the estimation of white matter and pial surfaces from intensity gradients, which are used to estimate cortical thickness. These cortical surfaces are projected into a common space (fsaverage) for comparison across individuals.

Brain MRI data has been used to predict age to study the brain aging process linked to diseases such as Alzheimer’s disease and Parkinson’s disease [29, 28, 10, 20, 35]. For the case studies based on the preprocessed ABIDE data [6, 2] in Section 3.2, we choose age at the MRI scan as the continuous outcome and autism diagnosis as the binary outcome. When using age at the MRI scan as the outcome, we adjust for sex and autism diagnosis; we using autism diagnosis as the outcome, we adjust for age and sex. We compare the few screening methods in our Python package `fastHDMI`, including mutual information estimation using the FFTKDE and k NN originally implemented in the `scikit-learn` library, as well as Pearson correlation.

3.1 Simulation based on the preprocessed ABIDE data [6, 2]

We decided to simulate outcomes based on the preprocessed ABIDE MRI features in order to preserve the distribution patterns and the correlation structure in this high-dimensional dataset. Therefore, we simulated both nonlinear and linear outcomes from the preprocessed ABIDE data [6, 2]. Let $\mathbf{X} \in \mathbb{R}^{N \times p}$ denote the design matrix; i.e., all the MRI brain imaging variables from the entire preprocessed ABIDE dataset. The simulation of the *nonlinear* outcomes proceeds in this manner – the nonlinearity for continuous outcomes comes from the quadratic manipulation, i.e., step 4:

1. Pick the number of “true” covariates p_{true} , choose p_{true} uniformly randomly from the full feature set; let $\mathbf{X}_{\text{true}} \in \mathbb{R}^{N \times p_{\text{true}}}$ denote the corresponding design sub-matrix.
2. Simulate the corresponding “true” coefficients $\boldsymbol{\beta}_{\text{true}} \in \mathbb{R}^{p_{\text{true}}}$ with $\boldsymbol{\beta}_{\text{true}} \sim N_{p_{\text{true}}}(1, \Sigma_{\boldsymbol{\beta}_{\text{true}}})$ and $\Sigma_{\boldsymbol{\beta}_{\text{true}}}$ being a 0.6 Toeplitz matrix. The correlation design aims to replicate the phenomenon of correlated brain signals.
3. Standardize the design sub-matrix for the true features \mathbf{X}_{true} , to obtain $\mathbf{X}_{\text{true},1}$.
4. For nonlinear simulations only: take the element-wise square of $\mathbf{X}_{\text{true},1}$ and then standardize the matrix again to obtain $\mathbf{X}_{\text{true},2}$; the standardization here is to ensure that each feature impacts the simulated outcome proportionally.
5. The continuous and binary outcomes are then simulated in this manner:
 - (a) To simulate continuous outcomes:
 - (i) Pick $\text{SNR} = 3$; calculate $\sigma_{\text{true}} = \sqrt{\frac{\boldsymbol{\beta}_{\text{true}}^T \mathbf{X}_{\text{true},2}^T \mathbf{X}_{\text{true},2} \boldsymbol{\beta}_{\text{true}}}{\text{SNR}}}$;
 - (ii) Simulate the error $\varepsilon_j \stackrel{i.i.d.}{\sim} N(0, \sigma_{\text{true}}^2)$;
 - (iii) The outcome is simulated as $\mathbf{y} = \mathbf{X}_{\text{true},2} \boldsymbol{\beta}_{\text{true}} + \boldsymbol{\varepsilon}$.
 - (b) To simulate binary outcomes:
 - (i) Calculate $\boldsymbol{\tau} = \mathbf{X}_{\text{true},2} \boldsymbol{\beta}_{\text{true}}$;
 - (ii) Standardize $\boldsymbol{\tau}$, obtain $\boldsymbol{\tau}'$ – this is to avoid the data being too centered, which will cause all simulated binary outcomes in the same class;
 - (iii) Take $\boldsymbol{\tau}'' = \boldsymbol{\tau}' + \text{arctanh}\sqrt{\frac{1}{3}}$ for *translated* binary outcome simulations, or $\boldsymbol{\tau}'' = \boldsymbol{\tau}'$ for *original* binary outcome simulations. The translated binary outcome simulation is to make the logistic transformation of centered data in the next step as nonlinear as possible, as $\pm \text{arctanh}\sqrt{\frac{1}{3}}$ is the location for the logistic transformation to achieve the greatest absolute curvature value;
 - (iv) The binary outcome is then simulated as $y_j \stackrel{\text{indep.}}{\sim} \text{Bern}(\text{logistic}(\tau_j''))$.

For linear simulations, we omit step 4 and take $\mathbf{X}_{\text{true},2} := \mathbf{X}_{\text{true},1}$ thereafter.

The screening of features with respect to the simulated continuous and binary outcomes \mathbf{y} are then carried out using the original entire design matrix \mathbf{X} . Variable selection performance is measured by *Variable Selection Area under Receiver Operating Curve (AUROC)*, which is the AUROC calculated with the true labels taking value 1 for the simulated true coefficients and 0 for other coefficients, and the ranking of the coefficients follows the absolute value of the three association measures, respectively; i.e., \widehat{MI} based on FFKDE and $k\text{NN}$, as well as Pearson correlation. The top p_{true} of the most associated covariates are then taken as selected covariates, which will take value 1, and the others will take value 0. Variable Selection AUROC therefore measures the matching between the selected covariates and the simulated “true” covariates. Such measures can differentiate distinct methods when the traditional measures such

as classification rate or adjusted Rand Index can not – a scenario frequently occurs to variable selection for ultra-high-dimensional data.

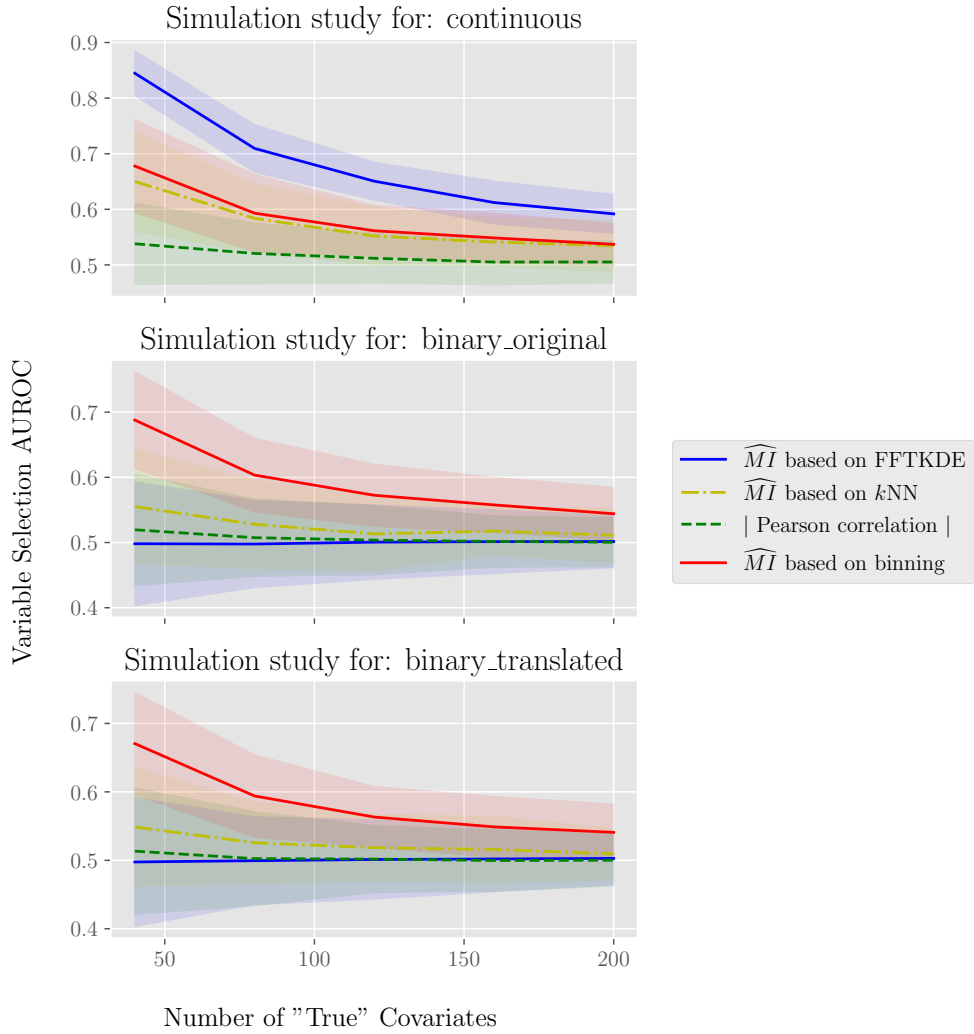


Fig. 1 Variable selection AUROC on the simulated *nonlinear* continuous and original/translated binary outcomes; the horizontal axis is the number of “true” covariates used in the outcome simulation. Means with their 95% confidence intervals were plotted for 100 simulation replications.

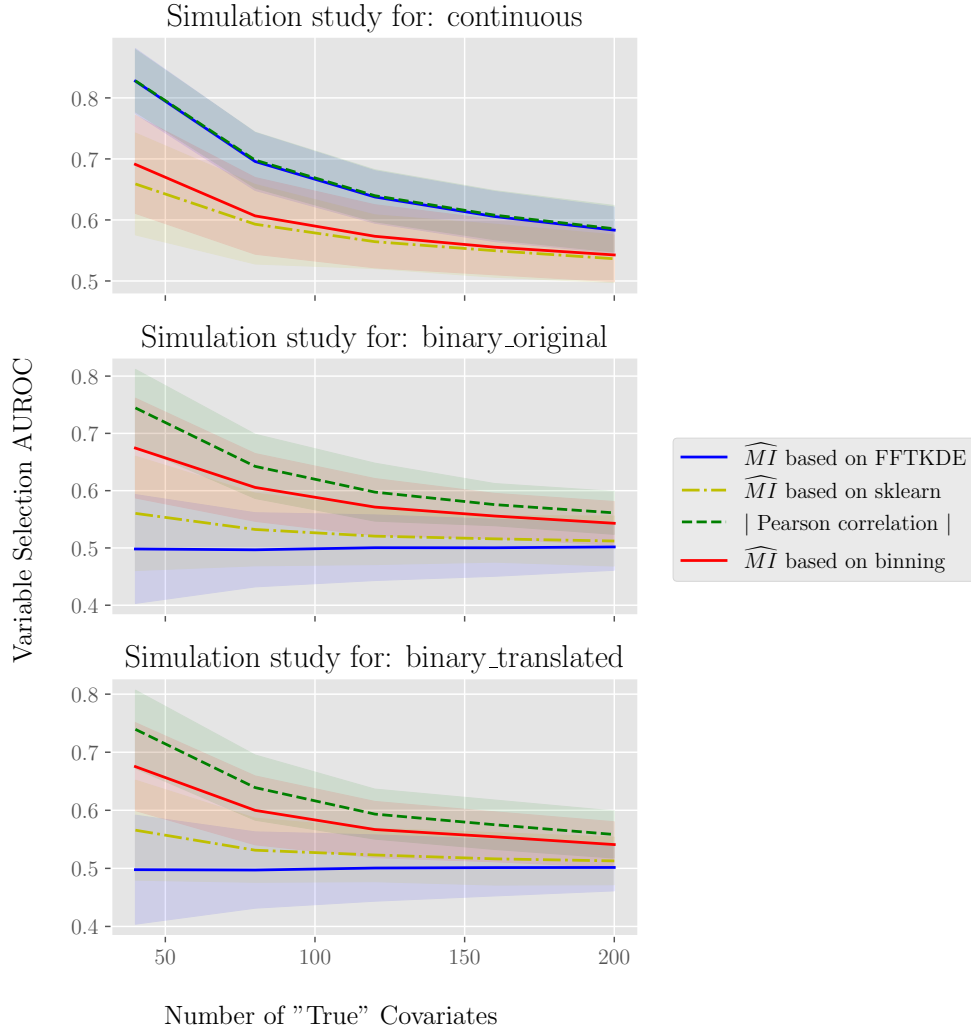


Fig. 2 Variable selection AUROC on the simulated *linear* continuous and original/translated binary outcomes; the horizontal axis is the number of “true” covariates used in the outcome simulation. Means with their 95% confidence intervals were plotted for 100 simulation replications.

We evaluate the efficacy of our implemented variable screening methods in `fastHDMI` package, including: 1) Mutual information estimation using FFTKDE, 2) Mutual information estimation using k NN, 3) Mutual information estimation through binning, and 4) absolute Pearson correlation. Our findings, illustrated in Figures 1 and 2, reveal that for continuous outcomes, the FFTKDE-based mutual information estimator outperforms its counterparts. In scenarios with linear relationships, FFTKDE-based mutual information estimator and absolute Pearson correlation are jointly the most effective. Conversely, for binary outcomes, the binning-based

mutual information estimator excels in capturing nonlinear associations, whereas other methodologies display substantially overlapping confidence intervals. In linear association contexts, Pearson correlation emerges as the most effective method for binary outcomes. Interestingly, Pearson correlation, particularly when employed with a balanced number of cases and controls, inherently correlates to a two-sample testing approach, which explains its superior performance for binary outcomes with linearly simulated underlying probability pre-image.

All discussed variable screening methods were conducted concurrently on 16-core CPUs on Compute Canada. The fast Fourier transform (FFT) algorithm is leveraged to significantly enhance the efficiency of the KDE estimation process, traditionally viewed as computationally intensive. As depicted in Figure 3, the execution times to complete the screenings with all the methods implemented in our `fastHDMI` package are assessed. Notably, the KDE-based mutual information estimation, often anticipated to be slower, exhibited competitive speed akin to alternative methods, courtesy of the FFT algorithm’s effectiveness. This computational efficiency was achieved with the same CPU configuration, while intentionally avoiding multiple data duplications in memory during multiprocessing. Given the substantial size of high-dimensional datasets, duplicating such datasets in memory is generally impractical.

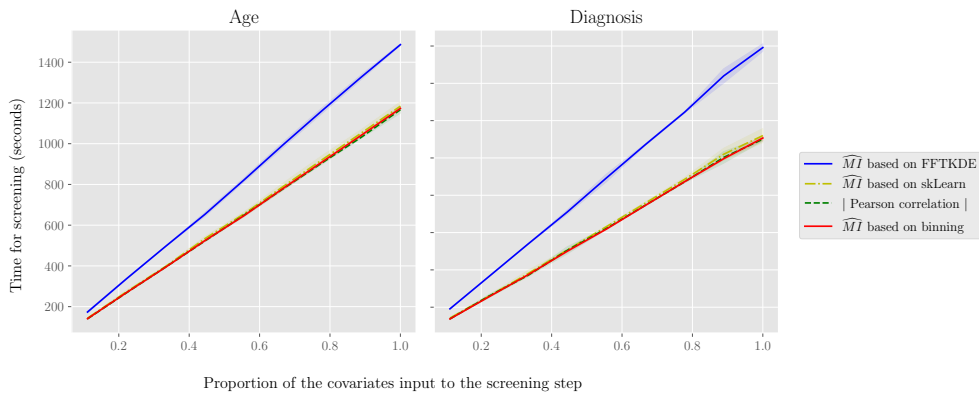


Fig. 3 Running speeds of variable screening for continuous (age) and binary (diagnosis) outcomes utilizing the methods under study. The horizontal axis represents the proportion of features introduced into the screening phase, while the vertical axis measures the time in seconds to complete the screening. The plot displays the mean running times and their corresponding 95% confidence intervals (C.I.), derived from 5 simulation replications.

3.2 Preprocessed ABIDE data case studies [6, 2] – predict age and diagnosis

In this subsection, we evaluate the performance of various variable screening techniques implemented in the `fastHDMI` package using preprocessed ABIDE data [6, 2]. Initially, we deploy the four variable screening methods to identify the features most associated with the outcome. Since we are fitting multiple penalized models, standardization of the selected variables is carried out to achieve a sample mean of 0 and a

standard deviation of 1. This step is crucial for ensuring consistent penalization across all coefficients of the penalized covariates.

Subsequently, we divide the dataset, stratified by the outcome, into a training set comprising 80% of the observations and a testing set with the remaining 20%. This stratification ensures a balanced representation of the outcomes in both sets. For the continuous outcome, age, we employ binning to categorize observations into 30 bins based on their outcome values, followed by stratification based on the bin labels. This approach allows for the division of the dataset into training and testing sets with similar outcome means, an important factor for reliable prediction performance comparison.

For the continuous outcome variable, age at MRI scan, we fit several models: elastic net, least-angle regression (LARS), least absolute shrinkage and selection operator (LASSO), LASSO-LARS, linear model, Random Forest regressor, and ridge regression. Except for the Random Forest regressor, which utilizes the out-of-bag error scored by R^2 for model averaging, all models are tuned using 5-fold cross-validation with validation set R^2 as the scoring function for penalty hyperparameters.

For binary outcomes, diagnosis of autism disorder, we fit both unpenalized and penalized logistic regressions (using ℓ_1 , ℓ_2 , and elastic net penalties), as well as the Random Forest classifier. All models, with the exception of the Random Forest classifier, which uses out-of-bag error scored by Gini impurity for model averaging, are tuned using 5-fold cross-validation, scored by mean accuracy for the penalty hyperparameters.

Unlike simulation studies in Section 3.1, where “true” signals are known, case studies lack such definitive benchmarks, necessitating reliance on model-based performance metrics. Hence, we use testing set R^2 for continuous outcomes and testing set Area Under the Receiver Operating Characteristic (AUROC) for binary outcomes to evaluate model performance.

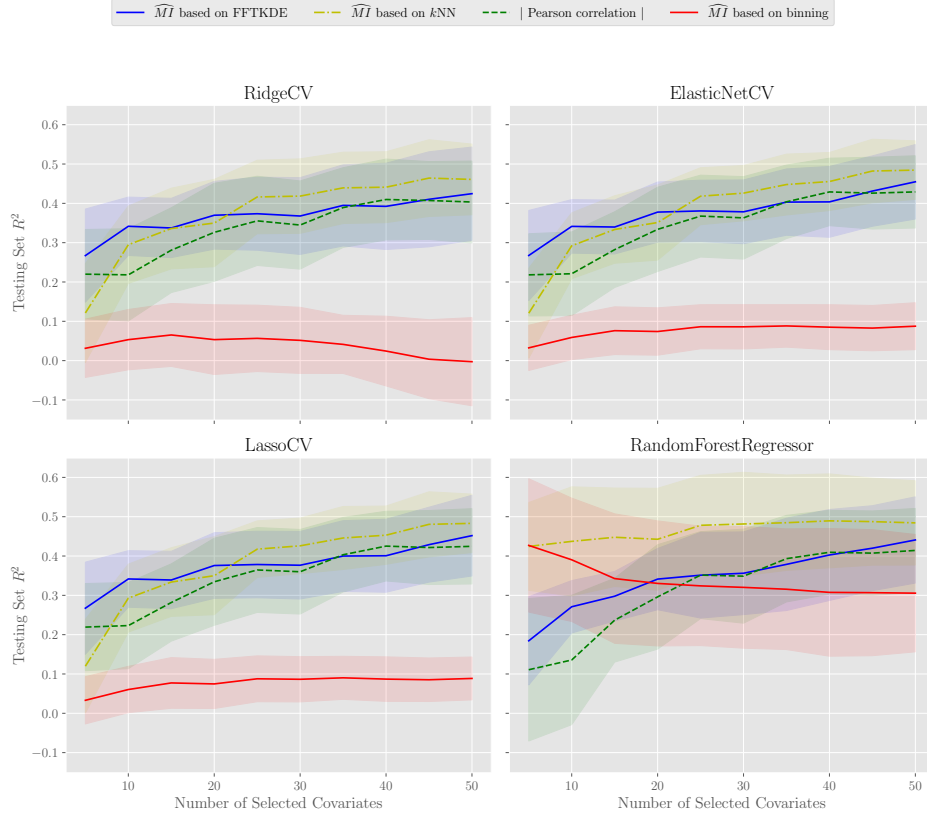


Fig. 4 Testing Set R^2 for age at the scan outcome v.s. the number of most associated brain imaging covariates based on the association measure rankings. Means with their 95% confidence intervals were plotted for 20 simulation replications.

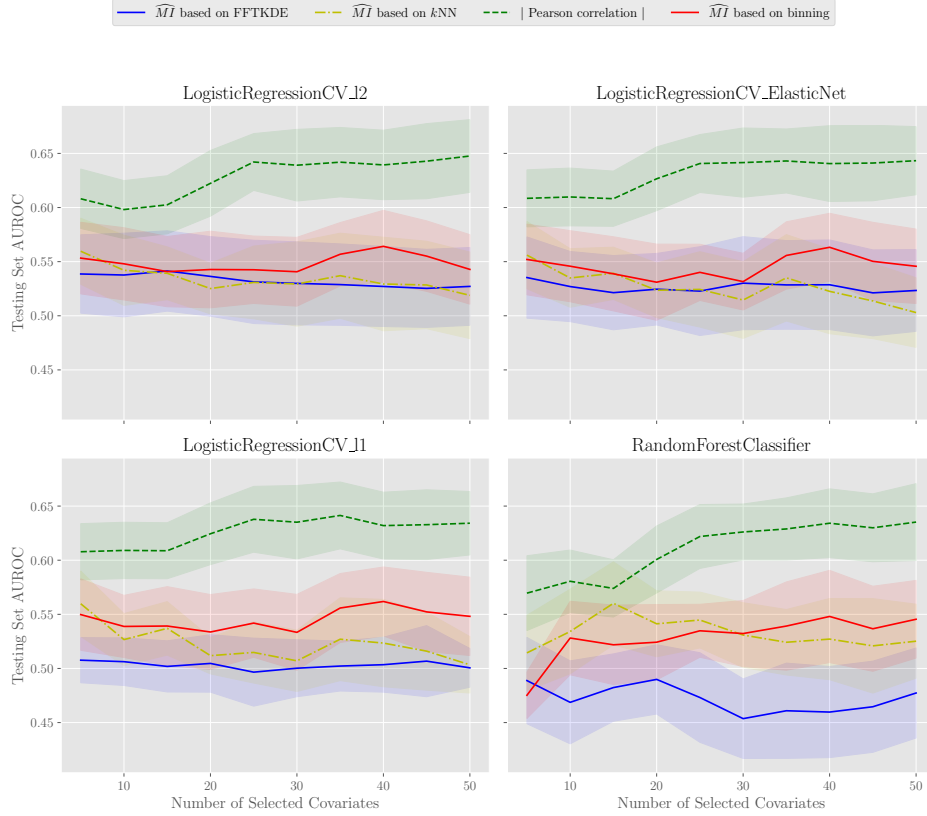


Fig. 5 Testing Set AUROC for autism diagnosis outcome v.s. the number of most associated brain imaging covariates based on the association measure rankings. Means with their 95% confidence intervals were plotted for 20 simulation replications.

Figure 4 illustrates that in predicting the continuous outcome, age at MRI scan, linear models utilizing brain imaging variables selected using mutual information estimations via FFTKDE or k NN emerge as the best-performing. Conversely, models built using variables selected by mutual information estimations based on binning exhibit the least predictive capability. However, within the context of random forest regression, models built using variables chosen through mutual information estimation by k NN outperform the rest. Figure 5 indicates that for the binary outcome of autism diagnosis, models constructed with variables selected via absolute Pearson correlation yield superior predictive performance. This phenomenon could stem from multiple factors, including the linear nature of the assessment model, which favors linear association measures, or a linear relationship between age at MRI scan, the probability of autism diagnosis, and the brain imaging covariates.

4 Conclusion and Discussion

In this paper, we introduce the Python package `fastHDMI`, designed to streamline variable screening through three distinct mutual information estimation methods along with absolute Pearson correlation. Our evaluations, conducted on the large, high-dimensional preprocessed ABIDE data [6, 2], affirm `fastHDMI`'s computational efficiency and robustness. Through extensive simulation studies, which encompass both simulations for linear and nonlinear associations, as well as continuous and binary simulated outcomes, we evaluated the performance of each implemented variable screening method. Our findings reveal that for simulated continuous nonlinear outcomes, the FFTKDE-based mutual information estimation method excels in variable selection. Similarly, for simulated binary outcomes with a nonlinear underlying probability preimage, the binning-based mutual information estimation stands out. In the cases of simulated continuous linear outcomes, both absolute Pearson correlation and FFTKDE-based mutual information estimation share the top performance. Furthermore, absolute Pearson correlation is superior for binary outcomes simulated with linear underlying probability preimage. Complementing our simulations, a comprehensive case study on the preprocessed ABIDE data [6, 2] showcased the predictive capabilities of models crafted from the most relevant covariates identified by our methods. By pioneering sophisticated variable selection techniques in the domain of high-dimensional neuroimaging data, our work stands as a critical advancement, fostering novel pathways for research exploration and analytical insight within the scientific community. A promising avenue for future research could be to explore variable screening based on non-parametric copula models [46].

5 Disclaimer

All codes to reproduce the simulation and case study results of this paper and outputs from Calcul Quebec/Compute Canada can be found on the following GitHub repository:

<https://github.com/Kaiyangshi-Ito/fastHDMI>

6 Acknowledgments

This work was supported by the ISM Scholarship for Outstanding PhD Candidates awarded to K. Yang, the NSERC Discovery Grant to C. Greenwood (Grant Number: RGPIN-2019-04482), the NSERC Discovery Grant to M. Asgharian (Grant Number: RGPIN-2024-05640), and the CANSSI Collaborative Research Team Grant to C. Greenwood and G. Cohen Freue.

References

- [1] Ehsan Adeli et al. "Kernel-based Joint Feature Selection and Max-Margin Classification for Early Diagnosis of Parkinson's Disease". In: *Scientific Reports* 7.1 (Jan. 2017). DOI: [10.1038/srep41069](https://doi.org/10.1038/srep41069).

- [2] Amadou Barry et al. “Asymmetric influence measure for high dimensional regression”. In: *Communications in Statistics - Theory and Methods* 51.16 (Nov. 2020), pp. 5461–5487. DOI: [10.1080/03610926.2020.1841793](https://doi.org/10.1080/03610926.2020.1841793).
- [3] Daniel Bell and Zach Drew. *Voxel size*. Sept. 2018. DOI: [10.53347/rid-62838](https://doi.org/10.53347/rid-62838).
- [4] Lucien Birgé and Yves Rozenholc. “How many bins should be put in a regular histogram”. In: *ESAIM: Probability and Statistics* 10 (Jan. 2006), pp. 24–45. ISSN: 1262-3318. DOI: [10.1051/ps:2006001](https://doi.org/10.1051/ps:2006001).
- [5] Z. I. Botev, J. F. Grotowski, and D. P. Kroese. “Kernel density estimation via diffusion”. In: *The Annals of Statistics* 38.5 (Oct. 2010). DOI: [10.1214/10-aos799](https://doi.org/10.1214/10-aos799).
- [6] Craddock Cameron et al. “The Neuro Bureau Preprocessing Initiative: open sharing of preprocessed neuroimaging data and derivatives”. In: *Frontiers in Neuroinformatics* 7 (2013). DOI: [10.3389/conf.fninf.2013.09.00041](https://doi.org/10.3389/conf.fninf.2013.09.00041).
- [7] Gwénaëlle Castellan. “Sélection d’histogrammes à l’aide d’un critère de type Akaike”. In: *Comptes Rendus de l’Académie des Sciences - Series I - Mathematics* 330.8 (Apr. 2000), pp. 729–732. ISSN: 0764-4442. DOI: [10.1016/s0764-4442\(00\)00250-0](https://doi.org/10.1016/s0764-4442(00)00250-0).
- [8] Barry Chai et al. “Exploring Functional Connectivity of the Human Brain Using Multivariate Information Analysis”. In: *Proceedings of the 22nd International Conference on Neural Information Processing Systems*. NIPS’09. Vancouver, British Columbia, Canada: Curran Associates Inc., 2009, pp. 270–278. ISBN: 9781615679119.
- [9] Girish Chandrashekar and Ferat Sahin. “A survey on feature selection methods”. In: *Computers & Electrical Engineering* 40.1 (Jan. 2014), pp. 16–28. DOI: [10.1016/j.compeleceng.2013.11.024](https://doi.org/10.1016/j.compeleceng.2013.11.024).
- [10] J H Cole et al. “Brain age predicts mortality”. In: *Molecular Psychiatry* 23.5 (Apr. 2017), pp. 1385–1392. DOI: [10.1038/mp.2017.62](https://doi.org/10.1038/mp.2017.62).
- [11] D. Louis Collins et al. “Automatic 3D Intersubject Registration of MR Volumetric Data in Standardized Talairach Space”. In: *Journal of Computer Assisted Tomography* 18 (1994), pp. 192–205. URL: <https://api.semanticscholar.org/CorpusID:8026836>.
- [12] Etienne Combrisson et al. “Group-level inference of information-based measures for the analyses of cognitive brain networks from neurophysiological data”. In: *NeuroImage* 258 (Sept. 2022), p. 119347. DOI: [10.1016/j.neuroimage.2022.119347](https://doi.org/10.1016/j.neuroimage.2022.119347).
- [13] James W. Cooley and John W. Tukey. “An algorithm for the machine calculation of complex Fourier series”. In: *Mathematics of Computation* 19.90 (1965), pp. 297–301. ISSN: 1088-6842. DOI: [10.1090/s0025-5718-1965-0178586-1](https://doi.org/10.1090/s0025-5718-1965-0178586-1).
- [14] Anders M. Dale, Bruce Fischl, and Martin I. Sereno. “Cortical Surface-Based Analysis”. In: *NeuroImage* 9.2 (Feb. 1999), pp. 179–194. ISSN: 1053-8119. DOI: [10.1006/nimg.1998.0395](https://doi.org/10.1006/nimg.1998.0395).
- [15] V. A. Epanechnikov. “Non-Parametric Estimation of a Multivariate Probability Density”. In: *Theory of Probability & Its Applications* 14.1 (Jan. 1969), pp. 153–158. ISSN: 1095-7219. DOI: [10.1137/1114019](https://doi.org/10.1137/1114019).
- [16] Lev Faivishevsky and Jacob Goldberger. “ICA Based on a Smooth Estimation of the Differential Entropy”. In: *Proceedings of the 21st International Conference on*

- Neural Information Processing Systems*. NIPS'08. Vancouver, British Columbia, Canada: Curran Associates Inc., 2008, pp. 433–440. ISBN: 9781605609492.
- [17] Miaolin Fan and Chun-An Chou. “Exploring stability-based voxel selection methods in MVPA using cognitive neuroimaging data: a comprehensive study”. In: *Brain Informatics* 3.3 (Apr. 2016), pp. 193–203. DOI: [10.1007/s40708-016-0048-0](https://doi.org/10.1007/s40708-016-0048-0).
 - [18] Elsa Santos Febles et al. “Machine Learning Techniques for the Diagnosis of Schizophrenia Based on Event-Related Potentials”. In: *Frontiers in Neuroinformatics* 16 (July 2022). DOI: [10.3389/fninf.2022.893788](https://doi.org/10.3389/fninf.2022.893788).
 - [19] Bruce Fischl. “FreeSurfer”. In: *NeuroImage* 62.2 (Aug. 2012), pp. 774–781. ISSN: 1053-8119. DOI: [10.1016/j.neuroimage.2012.01.021](https://doi.org/10.1016/j.neuroimage.2012.01.021).
 - [20] Katja Franke et al. “Estimating the age of healthy subjects from T1-weighted MRI scans using kernel methods: Exploring the influence of various parameters”. In: *NeuroImage* 50.3 (Apr. 2010), pp. 883–892. DOI: [10.1016/j.neuroimage.2010.01.005](https://doi.org/10.1016/j.neuroimage.2010.01.005).
 - [21] Shuyang Gao, Greg Ver Steeg, and Aram Galstyan. “Efficient Estimation of Mutual Information for Strongly Dependent Variables”. In: (Nov. 2014).
 - [22] Vanessa Gómez-Verdejo, Emilio Parrado-Hernández, and Jussi Tohka. “Sign-Consistency Based Variable Importance for Machine Learning in Brain Imaging”. In: *Neuroinformatics* 17.4 (Mar. 2019), pp. 593–609. DOI: [10.1007/s12021-019-9415-3](https://doi.org/10.1007/s12021-019-9415-3).
 - [23] Xiaoke Hao et al. “Multi-modal neuroimaging feature selection with consistent metric constraint for diagnosis of Alzheimer’s disease”. In: *Medical Image Analysis* 60 (Feb. 2020), p. 101625. DOI: [10.1016/j.media.2019.101625](https://doi.org/10.1016/j.media.2019.101625).
 - [24] Kevin He, Han Xu, and Jian Kang. “A Selective Overview of Feature Screening Methods with Applications to Neuroimaging Data”. In: *WIREs Computational Statistics* 11.2 (Sept. 2018). DOI: [10.1002/wics.1454](https://doi.org/10.1002/wics.1454).
 - [25] Megan J. Olson Hunt et al. “A variant of sparse partial least squares for variable selection and data exploration”. In: *Frontiers in Neuroinformatics* 8 (2014). DOI: [10.3389/fninf.2014.00018](https://doi.org/10.3389/fninf.2014.00018).
 - [26] Robin A.A. Ince et al. “A Statistical Framework for Neuroimaging Data Analysis Based on Mutual Information Estimated Via a Gaussian Copula”. In: *Human Brain Mapping* 38.3 (Nov. 2016), pp. 1541–1573. DOI: [10.1002/hbm.23471](https://doi.org/10.1002/hbm.23471).
 - [27] Ilinka Ivanoska et al. “Statistical and Machine Learning Link Selection Methods for Brain Functional Networks: Review and Comparison”. In: *Brain Sciences* 11.6 (May 2021), p. 735. DOI: [10.3390/brainsci11060735](https://doi.org/10.3390/brainsci11060735).
 - [28] Huiting Jiang et al. “Predicting Brain Age of Healthy Adults Based on Structural MRI Parcellation Using Convolutional Neural Networks”. In: *Frontiers in Neurology* 10 (Jan. 2020). DOI: [10.3389/fneur.2019.01346](https://doi.org/10.3389/fneur.2019.01346).
 - [29] B. A. Jonsson et al. “Brain age prediction using deep learning uncovers associated sequence variants”. In: *Nature Communications* 10.1 (Nov. 2019). DOI: [10.1038/s41467-019-13163-9](https://doi.org/10.1038/s41467-019-13163-9).
 - [30] Shiraj Khan et al. “Relative performance of mutual information estimation methods for quantifying the dependence among short and noisy data”. In: *Physical Review E* 76.2 (Aug. 2007), p. 026209. DOI: [10.1103/physreve.76.026209](https://doi.org/10.1103/physreve.76.026209).

- [31] Alexander Kraskov, Harald Stögbauer, and Peter Grassberger. “Estimating mutual information”. In: *Physical Review E* 69.6 (June 2004), p. 066138. DOI: [10.1103/physreve.69.066138](https://doi.org/10.1103/physreve.69.066138).
- [32] N. N. Leonenko L. F. Kozachenko. “Sample Estimate of the Entropy of a Random Vector”. In: *Probl. Peredachi Inf.* 23.2 (1987), pp. 9–16. URL: <http://mathscinet.ams.org/mathscinet-getitem?mr=908626>.
- [33] Qiang Li. “Functional connectivity inference from fMRI data using multivariate information measures”. In: *Neural Networks* 146 (Feb. 2022), pp. 85–97. DOI: [10.1016/j.neunet.2021.11.016](https://doi.org/10.1016/j.neunet.2021.11.016).
- [34] Zifei Liang et al. “Virtual mouse brain histology from multi-contrast MRI via deep learning”. In: *eLife* 11 (Jan. 2022). ISSN: 2050-084X. DOI: [10.7554/elife.72331](https://doi.org/10.7554/elife.72331).
- [35] Franziskus Liem et al. “Predicting brain-age from multimodal imaging data captures cognitive impairment”. In: *NeuroImage* 148 (Mar. 2017), pp. 179–188. DOI: [10.1016/j.neuroimage.2016.11.005](https://doi.org/10.1016/j.neuroimage.2016.11.005).
- [36] Kristin A. Linn et al. “Addressing Confounding in Predictive Models with an Application to Neuroimaging”. In: *The International Journal of Biostatistics* 12.1 (May 2016), pp. 31–44. DOI: [10.1515/ijb-2015-0030](https://doi.org/10.1515/ijb-2015-0030).
- [37] Warren M. Lord, Jie Sun, and Erik M. Bollt. “Geometric k-nearest neighbor estimation of entropy and mutual information”. In: *Chaos: An Interdisciplinary Journal of Nonlinear Science* 28.3 (Mar. 2018). DOI: [10.1063/1.5011683](https://doi.org/10.1063/1.5011683).
- [38] Cesare Magri et al. “A toolbox for the fast information analysis of multiple-site LFP, EEG and spike train recordings”. In: *BMC Neuroscience* 10.1 (July 2009). DOI: [10.1186/1471-2202-10-81](https://doi.org/10.1186/1471-2202-10-81).
- [39] Federico De Martino et al. “Combining multivariate voxel selection and support vector machines for mapping and classification of fMRI spatial patterns”. In: *NeuroImage* 43.1 (Oct. 2008), pp. 44–58. DOI: [10.1016/j.neuroimage.2008.06.037](https://doi.org/10.1016/j.neuroimage.2008.06.037).
- [40] J. Mohr et al. “P-SVM Variable Selection for Discovering Dependencies Between Genetic and Brain Imaging Data”. In: *The 2006 IEEE International Joint Conference on Neural Network Proceedings*. IEEE, 2006. DOI: [10.1109/ijcnn.2006.247207](https://doi.org/10.1109/ijcnn.2006.247207).
- [41] Young-Il Moon, Balaji Rajagopalan, and Upmanu Lall. “Estimation of mutual information using kernel density estimators”. In: *Physical Review E* 52.3 (Sept. 1995), pp. 2318–2321. DOI: [10.1103/physreve.52.2318](https://doi.org/10.1103/physreve.52.2318).
- [42] Idan E. Nemirovsky et al. “An Implementation of Integrated Information Theory in Resting-State fMRI”. In: *Communications Biology* 6.1 (July 2023). DOI: [10.1038/s42003-023-05063-y](https://doi.org/10.1038/s42003-023-05063-y).
- [43] Tommy Odland. *tommyod/KDEpy: Kernel Density Estimation in Python*. en. 2018. DOI: [10.5281/ZENODO.2392268](https://doi.org/10.5281/ZENODO.2392268).
- [44] Dávid Pál, Barnabás Póczos, and Csaba Szepesvári. “Estimation of Rényi Entropy and Mutual Information Based on Generalized Nearest-Neighbor Graphs”. In: *Proceedings of the 23rd International Conference on Neural Information Processing Systems - Volume 2*. NIPS’10. Vancouver, British Columbia, Canada: Curran Associates Inc., 2010, pp. 1849–1857.

- [45] Ernesto Pereda et al. “The blessing of Dimensionality: Feature Selection outperforms functional connectivity-based feature transformation to classify ADHD subjects from EEG patterns of phase synchronisation”. In: *PLOS ONE* 13.8 (Aug. 2018). Ed. by Ruxandra Stoean, e0201660. DOI: [10.1371/journal.pone.0201660](https://doi.org/10.1371/journal.pone.0201660).
- [46] Yassir Rabhi and Taoufik Bouezmarni. “Nonparametric Inference for Copulas and Measures of Dependence Under Length-Biased Sampling and Informative Censoring”. In: *Journal of the American Statistical Association* 115.531 (June 2019), pp. 1268–1278. ISSN: 1537-274X. DOI: [10.1080/01621459.2019.1611586](https://doi.org/10.1080/01621459.2019.1611586).
- [47] A. Rényi. “On measures of dependence”. In: *Acta Mathematica Academiae Scientiarum Hungaricae* 10.3–4 (Sept. 1959), pp. 441–451. ISSN: 1588-2632. DOI: [10.1007/bf02024507](https://doi.org/10.1007/bf02024507).
- [48] David N. Reshef et al. “Detecting Novel Associations in Large Data Sets”. In: *Science* 334.6062 (Dec. 2011), pp. 1518–1524. ISSN: 1095-9203. DOI: [10.1126/science.1205438](https://doi.org/10.1126/science.1205438).
- [49] Arkaprava Roy. “Nonparametric Group Variable Selection with Multivariate Response for Connectome-Based Modeling of Cognitive Scores”. In: (Oct. 2021). DOI: [10.48550/ARXIV.2110.05641](https://doi.org/10.48550/ARXIV.2110.05641). arXiv: [2110.05641](https://arxiv.org/abs/2110.05641) [stat.ME].
- [50] A. Schlögl, C. Neuper, and G. Pfurtscheller. “Estimating the mutual information of an eeg-based brain-computer interface”. In: *Biomedical Engineering* 47.1-2 (2002), pp. 3–8.
- [51] C. E. Shannon. “A Mathematical Theory of Communication”. In: *Bell System Technical Journal* 27.3 (July 1948), pp. 379–423. DOI: [10.1002/j.1538-7305.1948.tb01338.x](https://doi.org/10.1002/j.1538-7305.1948.tb01338.x).
- [52] Tarek Sherif et al. “CBRAIN: a web-based, distributed computing platform for collaborative neuroimaging research”. In: *Frontiers in Neuroinformatics* 8 (May 2014). ISSN: 1662-5196. DOI: [10.3389/fninf.2014.00054](https://doi.org/10.3389/fninf.2014.00054).
- [53] B. W. Silverman. “Algorithm AS 176: Kernel Density Estimation Using the Fast Fourier Transform”. In: *Applied Statistics* 31.1 (1982), p. 93. DOI: [10.2307/2347084](https://doi.org/10.2307/2347084).
- [54] Tamar Sofer, Lee Dicker, and Xihong Lin. “Variable selection for high dimensional multivariate outcomes”. In: *Statistica Sinica* (2014). DOI: [10.5705/ss.2013.019](https://doi.org/10.5705/ss.2013.019).
- [55] Terry Speed. “A Correlation for the 21st Century”. In: *Science* 334.6062 (Dec. 2011), pp. 1502–1503. ISSN: 1095-9203. DOI: [10.1126/science.1215894](https://doi.org/10.1126/science.1215894).
- [56] Elias M. Stein. *Fourier Analysis: An Introduction*. Elias M. Ed. by Rami Shakarchi. 15. Druck. Vol. 1. Fourier analysis. Hier auch später erschienene, unveränderte Nachdrucke. Princeton: Princeton University Press, 2003. 309 pp. ISBN: 9780691113845.
- [57] R. Steuer et al. “The mutual information: Detecting and evaluating dependencies between variables”. In: *Bioinformatics* 18.suppl.2 (Oct. 2002), S231–S240. DOI: [10.1093/bioinformatics/18.suppl.2.s231](https://doi.org/10.1093/bioinformatics/18.suppl.2.s231).
- [58] Shruthi Suresh et al. “Feature Selection Techniques for a Machine Learning Model to Detect Autonomic Dysreflexia”. In: *Frontiers in Neuroinformatics* 16 (Aug. 2022). DOI: [10.3389/fninf.2022.901428](https://doi.org/10.3389/fninf.2022.901428).

- [59] Andy Tsai et al. “Analysis of Functional MRI Data Using Mutual Information”. In: *Medical Image Computing and Computer-Assisted Intervention – MICCAI’99*. Springer Berlin Heidelberg, 1999, pp. 473–480. DOI: [10.1007/10704282_51](https://doi.org/10.1007/10704282_51).
- [60] Jonathan D. Victor. “Binless strategies for estimation of information from neural data”. In: *Physical Review E* 66.5 (Nov. 2002), p. 051903. DOI: [10.1103/physreve.66.051903](https://doi.org/10.1103/physreve.66.051903).

Appendix A Methodology Consideration

For a function f defined over an Euclidean space \mathbb{R}^n , its (continuous) Fourier transform is defined as

$$(\mathcal{F}f)(\xi) := \int_{\mathbb{R}^n} f(x) \exp(-2\pi i \cdot \langle x, \xi \rangle) dx, \quad (\text{A1})$$

a linear operator. The Fourier series is then the synthesis formula. Consider a square-integrable function space $L^2([-\pi, \pi])$, the fundamental results of Fourier analysis [56] conclude that $\{\phi_k := \exp(ikx) \mid k \in \mathbb{Z}\}$ is an orthonormal and complete basis for this Hilbert space with the inner product being defined by

$$\forall f, g \in L^2([-\pi, \pi]), \langle f, g \rangle := \frac{1}{2\pi} \int_{-\pi}^{\pi} f(x) \bar{g}(x) dx.$$

We remark that the inner product for a complex Hilbert space is linear for the first argument and anti-linear for the second argument. The Fourier series that represents any function $f \in L^2([-\pi, \pi])$ is then

$$f = \sum_{k=-\infty}^{\infty} \langle f, \phi_k \rangle \phi_k.$$

Clearly, (1D continuous) Fourier transform is to extend the idea of decomposing functions on the interval $[-\pi, \pi]$ to analyzing them across \mathbb{R} by scaling the frequency domain. This approach applies analogously to higher-dimensional situations. The completeness of the Fourier basis is given by the Fourier theorem, while the uniqueness of continuous Fourier transform and the inverse Fourier transform under certain conditions is a key result in Fourier analysis [56]. An important property of the Fourier series/continuous Fourier transform is the convolution property:

$$\forall f, g \in L^2([-\pi, \pi]), \mathcal{F}(f * g) = (\mathcal{F}f) \cdot (\mathcal{F}g),$$

where \mathcal{F} denotes the Fourier transform.

For a finite number of data points, *discrete Fourier transform (DFT)* can be used to approximate a function using the Fourier basis $\{\phi_k\}$ mentioned above. In the context of our discussion of DFT, for a slight abuse of notions, let \mathcal{F} also represent the Fourier series. In physical space, the equispaced grid of points is usually scaled first to match the domain of the DFT transform, often chosen as $[-\pi, \pi]$ for 1D data or

$[-\pi, \pi] \times [-\pi, \pi]$ for $2D$ data. DFT then transforms the function values evaluated at the equispaced data points in the physical space to Fourier coefficients in the frequency space by multiplication of the following matrix, called DFT matrix:

$$\Psi := N^{-\frac{1}{2}} \begin{bmatrix} \psi^0 & \psi^0 & \psi^0 & \dots & \psi^0 \\ \psi^0 & \psi & \psi^2 & & \psi^{N-1} \\ \psi^0 & \psi^2 & \psi^4 & & \psi^{2(N-1)} \\ & \vdots & & \ddots & \vdots \\ \psi^0 & \psi^{N-1} & \psi^{2(N-1)} & \dots & \psi^{(N-1)(N-1)} \end{bmatrix},$$

where $\psi := \exp(-\frac{1}{N}2\pi i)$. FFT is an algorithm to efficiently perform the DFT for a finite number of data points, reducing the complexity from $O(N^2)$ to $O(N \log N)$ [13]. Inverse FFT can be done similarly.

In a two-dimensional space, the DFT of the function f is based on the projection on a $2D$ Fourier basis $\{\phi_k := \exp(ikx + i jy) \mid k, j \in \mathbb{Z}\}$. The convolution property and FFT in a $2D$ space is then similar to that of the $1D$ space [56, 13].

Based on above, kernel density estimation can be computed efficiently using the convolution property of Fourier transform and FFT [53]. Silverman [53] further demonstrated the outstanding numerical performance of Fast Fourier Transform-based Kernel Density Estimation (FFTKDE). Specifically, the kernel density estimation for N data points is

$$\hat{f}(x; \Omega) := N^{-1} \sum_{j=1}^N K(x - x_j; \Omega),$$

where K denotes the kernel and Ω denotes the bandwidth matrix. Thus, KDE can be carried out efficiently by

$$\hat{f}(x; \Omega) = N^{-1} \sum_{j=1}^N K(x; \Omega) * \delta(x - x_j),$$

where δ is Dirac delta, which functions as a ‘‘spike’’ and has Fourier transform being a constant function depending only on the chosen normalization constant of the Fourier transform. This allows \hat{f} to be calculated efficiently, since the convolution property of Fourier transform implies that

$$\mathcal{F}(\hat{f})(x; \Omega) = \mathcal{F}(K)(x; \Omega) \cdot \mathcal{F}(\delta)(x - x_j).$$

Then, $\hat{f}(x; \Omega)$ evaluated on a $2D$ equispaced grid can be calculated using IFFT. Therefore, the evaluated density value on the $2D$ equispaced grid can be used to calculate the mutual information estimation, specifically,

$$\widehat{MI}(Y, X_j) = \int_{\text{supp}(Y)} \int_{\text{supp}(X_j)} \hat{f}_{Y, X_j}(y, x_j) \cdot \log \frac{\hat{f}_{Y, X_j}(y, x_j)}{\hat{f}_Y(y) \cdot \hat{f}_{X_j}(x_j)} dx_j dy \quad (\text{A2})$$

In (A2), $\hat{f}_Y(y)$, $\hat{f}_{X_j}(x_j)$, and the expectation estimator itself can be numerically computed using the forward Euler method. Notably, employing the FFT for the integration of density functions often fails to deliver satisfactory numerical results, primarily attributed to the inherent periodic characteristics of the method. (A2) is the equation that we use to calculate the FFTKDE mutual information estimator.

The estimation of mutual information using another nonparametric method, k NN [16, 31, 60, 44, 37, 21], was also discussed in the paper. The estimation of mutual information based on k NN can be viewed through the lens of k NN density estimator. The bivariate k NN density estimator can be given by

$$\hat{f}(x; k) := \frac{k}{N} \cdot (\pi \cdot R^2(x; k))^{-1},$$

where $R(x; k)$ denotes the Euclidean distance from x to its k -nearest-neighbor. In the context of a bivariate density estimator, $\pi \cdot R^2(x; k)$ represents the area of the Euclidean-normed closed ball centered at x that includes the k -nearest-neighbors of x . Following the idea of empirical CDF, the probability that a data point is included in this closed ball is $\frac{k}{N}$; assuming that the density inside the closed ball remains constant, the estimate of such density will be the probability of being included in the closed ball divided by the area of the closed ball, which is the bivariate density estimator described above. The multivariate case with more than two variables can be established in a similar way.